Teletraffic/Transmission Performance of Multi-Hop Networks using Hybrid-Store-and-Forward

G. A. Castañón, O. K. Tonguz and A. Bononi[1]

Abstract— The teletraffic/transmission performance of regular two-connected multi-hop cell-switching optical networks in uniform traffic under hybrid store-and-forward is presented. Manhattan Street (MS) Network and ShuffleNet (SN) are compared in terms of average queueing delay, queue size, transit delay, throughput, and bit error rate (BER) for intensity modulation/direct-detection (IM/DD) both analytically and by simulation. A hybrid semi-transparent store-and-forward node architecture is presented. Cells are electronically stored just in the case of conflict to avoid deflection, otherwise the cells will traverse the node without opto-electronic conversion. This architecture performs well, in terms of throughput, propagation delay and BER. It is also shown that by combining deflection routing with the store-and-forward scheme the network can accommodate two different bit-rates. This suggests that the proposed hybrid scheme may have good potential for future multimedia networks.

1. INTRODUCTION

The major advantage of cross-connected optical networks is that they achieve higher throughput than linear topologies like buses and rings [1], [2]. If buffers are not available, the cells can be temporarily deflected to an undesired link. Thus, deflection routing allows the use of fiber links as optical buffers [1]-[3] while *bit-rate non-regenerative transparency* is maintained. Such an advantage in traffic management causes a major weakness in transmission [4]. It has been shown [5] that the quality of signals decreases with traffic load due to accumulation of weak noises such as the amplifier spontaneous emission (ASE) noise and coherent crosstalk in high-speed transparent networks. Therefore, node architectures that limit the propagation delay to a minimum average number of hops and keep a certain bit-rate transparency are ideal for cross connected networks. Here we present and analyze one of such semi-transparent node architectures. Such an architecture avoids deflections by providing internal electronic buffers. Cells are stored just in the case of conflict, to avoid deflection, otherwise the cells will transparently traverse the node (transparent cut-through [6] routing). Buffered cells only are regenerated by the intermediate nodes.

We analyze the performance of this node architecture under two access schemes: a) buffered cells have access priority; b) locally generated cells have access priority. These two access schemes have a largely different impact on the queue size and, therefore, on the queueing delay. Also, we will show that this node architecture can sustain a two bit-rate communication if a combination of hybrid store-and-forward and deflection routing is used.

This paper analyzes the steady-state behavior of two connected mesh networks under a hybrid-store-and-forward (H-S&F) scheme. The analytical teletraffic model in [3] is reviewed and extended to H-S&F. Also, we present results of the transmission performance based on the *traffic randomness* of multi-hop cell-switched multiwavelength networks at the *optimal transmission power.* We present the limit of operation based on a *uniform traffic* scenario. The main impairments considered in the transmission analysis are intra-band crosstalk and ASE noise.

2. NODE STRUCTURE

The node is composed of a stack of submodules, one per each wavelength. The wavelengths from the input fibers are spatially demultiplexed and sent to the appropriate submodule for add/drop operations and switching. Cells from the submodules are finally re-multiplexed onto the output fibers. Fig. 1 shows a hybrid structure that employs two electronic buffers with sufficient capacity. The header recognition block taps power off to electronically read the cell header and make routing/control decisions. Each submodule is equipped with one transmitter (TX) and two receivers (RX). Cells transparently flow through the node and are stored only in case of conflict. This avoids both deflection and repetitive optical/electronic conversion (as in conventional S&F). Stored cells are transmitted assuming a first-in-first-out (FIFO) scheme. Buffered cells are regenerated by the intermediate nodes.

When a cell is routed through a node, one of the two outputs is chosen according to a shortest path algorithm [7]. Based on the position of the intermediate node and the cell's destination node, one or both outputs may be suitable for minimizing the number of hops a cell has to traverse for reaching destination. A cell that can take both outputs is called a *don't care cell,* while a cell that has only one preferred output is called a *care cell.* Basically, slots can be empty (E), can carry a cell for the node (FN), or a cell that cares to exit at output 1 (C1) or output 2 (C2), or a don't care (DC) cell.

Now let's briefly define some teletraffic parameters. Define u as the input slot utilization, i.e., the probability that an input slot carries a cell. Define P_{dc} as the probability that an incoming cell is DC. Let a be the probability that an input cell

[1] G. A. Castañón, O. K. Tonguz are with the Photonics Research Laboratory, Department of Electrical and Computer Engineering, State University of New York at Buffalo, Buffalo, NY 14260, USA. http://www.acsu.buffalo.edu/~castanon, http://www.acsu.buffalo.edu/~tonguz.

A. Bononi is with Dipartimento di Ingegneria dell'Informazione Università di Parma, I-43100 Parma ITALY. E-mail: alberto@com.tlc.unipr.it.

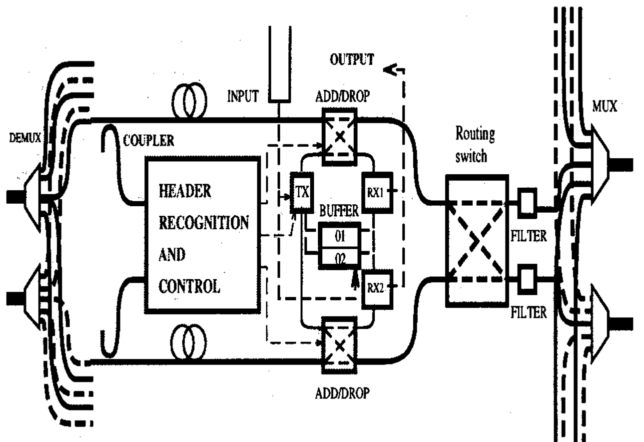

Figure 1: a) Node and submodule block diagram, submodule stores cells just in the case of conflict.

is destined to the node. The probability of cell absorption a is related to the average propagation delay H (in number of hops) as: $a = 1/H$ [3]. We will assume that, at every time-slot t, the input arrivals $i_1(t)$, $i_2(t)$ (of one wavelength) are independent random variables with the same probability distribution $\mathbf{f_i} = \{Pr[i_j = s], s \in \{E, FN, DC, C2, C1\}\}$, $j = 1, 2$. From the above definitions one gets after the absorption stage: $\mathbf{f_i} = \{f_i(E), f_i(FN), f_i(DC), f_i(C)\} = \{1 - u(1-a), ua, u(1-a)P_{dc}, u(1-a)(1-P_{dc})\}$ [3]. Also define $A0$, $A1$, and $A2$ as the probabilities of having respectively 0, 1 or 2 cells in one wavelength (or submodule) after the absorption stage, whose expressions are

$$\begin{aligned} A0 &= (1-u(1-a))^2 \\ A1 &= 2u(1-u)(1-a) + 2u^2a(1-a) \\ A2 &= u^2(1-a)^2. \end{aligned} \quad (1)$$

To keep the analysis simple, we assume that each TX has no local input queue. New cells per wavelength are generated in each time slot with probability g, the generation probability. If a new cell is generated but can not be injected into the network, local blocking occurs and the local cell is discarded.

3. ACCESS SCHEMES

We will assume that successive slot-by-slot arrivals are independent. This assumption is partially violated when use is made of buffers and the *access priority* is given to the newly *generated cells by the submodule* since, at high loads, the buffers tend to correlate successive arrivals [8], [9]. This successive cell correlation causes one of the buffers of a generic submodule to be filled at a faster rate than the other, thus generating imbalance in the queues and extra queue size and queueing delay. This successive cell correlation depends on the traffic load and affects ShuffleNet [8] at high traffic loads ($g > 0.7$) while Manhattan Street is little affected as we will show. However, when access priority is given to the routing buffers, the degree of correlation of successive arrivals is small for both SN and MS. Therefore, the model presented here, which assumes that the arrivals on different links are independent, is fairly accurate. We present simulation results to validate the accuracy of the model according to the method discussed in [10], which we extend to H-S&F.

3.1. Hybrid-S&F: Buffered cells have access priority

In this section we will derive the average queue size and the queueing delay when cells stored in the electronic routing buffers have access priority over cells generated by the submodule. The two queues (01 and 02) of Fig. 1 can be modeled as independent birth-death Markov chains, each with birth rate β and death rate μ. The average queue size (in number of cells) of one buffer is given by [11] $Q_b = \frac{\beta}{\mu-\beta}$, where

$$\beta = \frac{1}{2}\frac{[A2 + gq^2A1](1-P_{dc})^2}{2} \quad (2)$$

$$\begin{aligned} \mu &= (q + \frac{1-q}{2})(A0 + A1P_{dc}) + \frac{A1(1-P_{dc})}{2} \\ &+ \frac{1}{2}\frac{A2(1-P_{dc})^2}{2}. \end{aligned} \quad (3)$$

The symbols have the following meaning. β is the probability to store a cell in one buffer. A cell is stored just in the case that two care cells desire the same output link (to avoid deflection). This event will occur when there are two ($A2$) incoming care ($1 - P_{dc}$) cells at the links of the submodule, with the same output preference (1/2), or the submodule generates a new care cell whenever the buffers are empty (q^2) and there is one ($A1$) incoming care cell with the same output preference (1/2) as the locally generated cell. If this last event occurs, the locally generated cell is routed electronically to the buffers (see Fig. 1a) instead of storing the cell that is in transit. The first (1/2) factor in (2) is the probability to store a cell in buffer 01 or 02. μ is the probability of buffer transmission. This will occur if the second buffer is empty (q), or the second buffer is not empty and there is 1/2 probability of buffer selection and there are two free slots ($A0$) or one ($A1$) don't care cell is present (P_{dc}). The second term refers to the probability that one incoming care cell is present targeting the same output as the stored cell with probability 1/2. The last term refers to the probability that a cell is stored in the second buffer. Also in this case buffered cells have access priority over locally generated cells. Due to the symmetry of the networks, and considering that the traffic is uniform, we assume the same β, μ, and q for both queues of each submodule.

The probability that one of the buffers is empty (q), is given by [11] $q = \frac{\mu-\beta}{\mu}$, and the average queueing delay produced by one buffer is [11] $D_b = \frac{1}{\mu-\beta}$.

Applying Little's theorem to one optical channel of the network including the buffers, the balance equation is $\lambda H = 2\aleph u$, where λ is the network's per channel throughput, i.e. the average number of cells inserted/absorbed per slot per channel

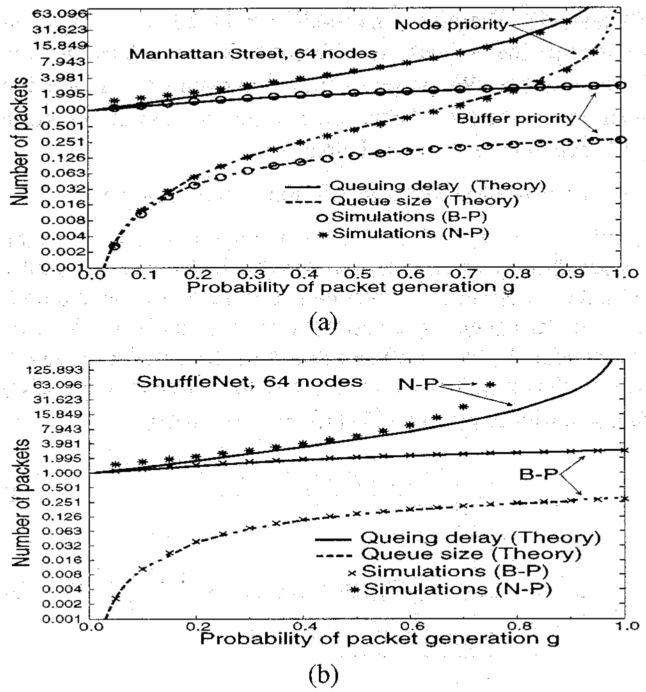

Figure 2: Queueing delay and Queue size in number of cells vs. g for a) Manhattan Street and b) ShuffleNet topologies with 64 nodes.

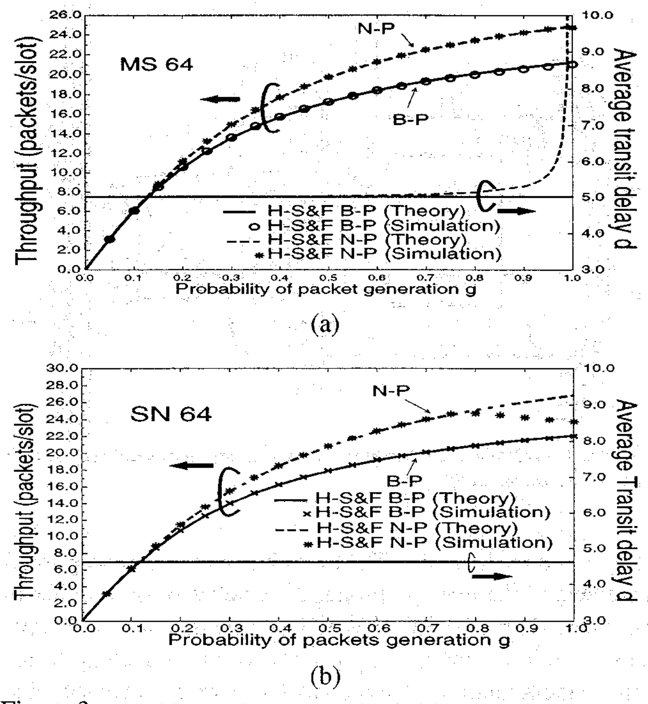

Figure 3: Throughput and Total network cell delay in number of hops vs. g for a) Manhattan Street and b) ShuffleNet topologies.

in the network at equilibrium. $\aleph$ is the number of submodules per channel.

The average number of newly transmitted (injected) cells per submodule is obtained as the probability of having a new cell ready for transmission (g) times the probability that both buffers are empty (q^2) times the probability that at least one of the two slots is free. Then, $\frac{\lambda}{\aleph} = gq^2(1-u^2(1-a)^2)$. It is easily seen that

$$u = \frac{\sqrt{a^2 + (gq^2)^2(1-a)^2} - a}{gq^2(1-a)^2}, \tag{4}$$

and the total average transit delay, that is the sum of the propagation delay H and the possible internal queueing delay normalized by the hop propagation delay, is $d = H(1 + \frac{D_b \rho}{W})$ where $W = \frac{l}{c/n}\frac{R}{M} \cong 11.75R[Gb/s]l[km]$ is the ratio of link length to the spatial length of one slot [3], where l is the link length, c/n is the light speed in optical fibers of refraction index $n = 1.5$, R is the bit rate and M the cell size (424 bits). $HD_b\rho$ is the possible queueing delay, where $\rho = \frac{1}{4}u(1-a)(1-P_{dc})^2$ is the probability of buffering a cell.

3.2. Hybrid-S&F: locally generated cells have access priority

In this section we will derive the average queue size and the average queueing delay for the case of Hybrid-S&F when cells generated by the submodule have access priority over cells stored in the buffers. In this case $\beta = \frac{1}{2}\frac{[A2+gA1](1-P_{dc})^2}{2}$ and $\mu = (q + \frac{1-q}{2})(1-g)(A0 + A1P_{dc}) + \frac{(1-g)A1(1-P_{dc})}{2} + \beta$, where β and μ can be obtained by reasoning as in equations (2) and (3), except that in this case β is not conditioned on the buffer being empty, and μ is conditioned on the probability that no new cells from the submodule are present for transmission $(1-g)$. In this case the link utilization u is given by $u = \frac{\sqrt{a^2+g^2(1-a)^2}-a}{g(1-a)^2}$.

The values of the average number of hops (H) and probability of don't care (P_{dc}) can be obtained considering a probability of cell deflection $p = 0$ (for this case) and that the random walk of a test cell toward destination is modeled as an absorbing Markov chain whose states are defined by the network nodes, the only absorbing state being the destination node as in [3], [12].

Fig. 2 shows the average queue size Q_b and the average queueing delay D_b in number of cells for MS and SN networks with 64 nodes. When access priority is given to the routing buffers (B-P) the average queue size is smaller than 1 cell and the average queueing delay is lower than 4 cells for both topologies. When access priority is given to locally generated cells (N-P) the queue size and queueing delay are reasonable for MS at loads lower than $g = 0.95$. Observe that theory and simulation results show a good agreement for MS topology, while results for SN (N-P) present a mismatch between the theory and simulation at loads higher than $g = 0.7$. The reason for this discrepancy is that buffers tend to correlate the cells and buffer imbalance is produced generating extra queue size and queueing delay.

Fig. 3 shows throughput and average transit delay d (in hops) versus probability of cell generation g for MS and SN topologies. When access priority is given to the locally generated cells (N-P) MS gives a high throughput; however, the average transit delay d increases at high loads ($g > 0.95$) due to queueing delays. For the case of SN the throughput given by the simulation starts to decay at $g = 0.75$ due to the fact that cell correlation produces a higher number of conflicts at the nodes, this means that more cells are stored/extracted in/from the buffers, therefore less new cells are injected and throughput decays. This fact indicates that cell correlation is much more severe in SN64 than in MS64. When access priority is given to the routing buffers (B-P) the throughput is $\lambda = 21$ for MS and $\lambda = 22.1$ for SN at $g = 1$. Also, the average transit delay is about 5 and 4.7 hops for MS and SN respectively, however this comes at expense of reducing the throughput with respect to N-P. Observe that the internal queueing delay is minimized because the internal buffers have access priority. The H-S&F average internal queueing delay of a generic cell during its travel to destination is given by $HD_b\rho$ cells (or slots). If one considers the worst case, in which a cell is successively stored at each node (then $\rho = 1$), the total internal buffer delay for B-P case is about 20 cells for MS and 19 cells for SN at **g=1**. Indeed, **g=1** corresponds to the case of a saturated infinite input queue at the transmitters [13].

3.3. Hybrid S&F-deflection routing: Transmission at two different bit rates

Now suppose that N_{R2} submodules on one optical channel want to upgrade their bit-rate to bit-rate-2 ($R2$) and N_{R1} submodules remain at bit-rate-1 ($R1$)($R2 > R1$). Assume, for analytical convenience, that $R2 = mR1$, where m is an integer. If a submodule that transmits at R2 wants to send a cell to a submodule that receives at bit-rate $R1$, it has to repeat ones or zeros m times each. Then the actual bit rate of the connection is R1. Conversely, if the transmission is from slow submodules $R1$ to fast submodules $R2$, the fast receiver, which integrates over its bit time $\frac{1}{R2}$, has to be able to collect m samples before making a decision. This is called oversampling, and has the effect of decreasing the error rate, even though the receiver has more noise because of the larger receiver bandwidth. However, we will assume the worst-case scenario in which $R1$ submodules communicate only with submodules of the same kind and the same holds for submodules of kind $R2$. If submodule cross-communication is considered, the results with respect to transit delay, throughput and buffer-size tend to be similar to those presented in the previous sections. Therefore, we will assume that: 1) the head of the cells is transmitted at one common bit-rate 1; 2) cells have the same spatial size; i.e. R2 cells will contain $m * M$ more bits than R1 cells; 3) each submodule transmit/receive/store at one bit rate only depending on its kind; 4) the submodules are uniformly distributed over the network. The total number of submodules per channel is $\aleph = N_{R1} + N_{R2}$. We will approximate the probability to find a cell in transit of bit-rate R1 (P_{p-R1}) to the probability that one submodule chosen at random receives/transmits at R1 (P_{n-R1}), so that $P_{p-R1} = P_{n-R1} = \frac{N_{R1}}{\aleph}$ and similarly for R2 cells.

If there is a conflict in a submodule that receives at a bitrate different from that of both cells, one of the cells is deflected, i.e. the probability that one R1 test cell is deflected at any submodule is $p_{R1} = \frac{P_c}{(2)(2)} P_{p-R1} P_{n-R2}$, where $P_c = u(1-a)(1-P_{dc})$ is the probability of having a care cell at the input of the routing switch (see Fig. 1) together with a R1 test cell at an intermediate care submodule. The first 1/2 refers to the probability of having two care cells with the same output preference, while the second 1/2 is the probability that one of the two cells is selected for deflection. P_{p-R1} is the probability that the second care cell is R1 and P_{n-R2} is the probability that the submodule reads at R2. Note that the probability that one R2 test cell be deflected is $p_{R2} = \frac{P_c}{(2)(2)} P_{p-R2} P_{n-R1}$ which is numerically the same as p_{R1}.

When the buffered cells have access priority (B-P), the probability to store a cell in one buffer of an R1 submodule β_{R1} and the probability of transmitting a cell from one buffer of an R1 submodule μ_{R1} is:

$$\beta_{R1} = \frac{(1-P_{dc})^2}{(2)(2)}[A2(2P_{p-R2}P_{p-R1} + P_{p-R1}^2) + gq_{R1}^2 A1] \quad (5)$$

$$\mu_{R1} = (q_{R1} + \frac{1-q_{R1}}{2})(A0 + A1P_{dc}) + \frac{A1(1-P_{dc})}{2} + \frac{1}{2}\frac{A2(1-P_{dc})^2}{2}. \quad (6)$$

An arrival β_{R1} will occur when there are two incoming care cells with the same output preference (1/2) and with different bit rate or with same bit rate R1 as the submodule's bit rate R1, or the submodule generates a new care cell whenever the buffers are empty and there is one incoming care cell with the same output preference (1/2). The second 1/2 in (5) is the probability to store the cell in buffer 01 or 02. μ_{R1} can be obtained reasoning as in (3) except that in this case $q_{R1} = \frac{\mu_{R1}-\beta_{R1}}{\mu_{R1}}$ is the probability that one of the buffers of a submodule that transmits/receives at R1 is empty. The probability β_{R2} and μ_{R2} can be obtained by reasoning as in expressions (5) and (6), and in this case $q_{R2} = \frac{\mu_{R2}-\beta_{R2}}{\mu_{R2}}$.

The average number of newly transmitted cells per submodule is obtained as the probability of having a new cell times the probability that both buffers of an R1 submodule are empty or both buffers of an R2 submodule are empty times the probability that at least one of the two slots is free. Then, $\frac{\lambda}{\aleph} = g\chi(1-u^2(1-a)^2)$, where $\chi = q_{R1}^2 P_{n-R1} + q_{R2}^2 P_{n-R2}$. For this case the link utilization is

$$u = \frac{\sqrt{a^2 + (g\chi)^2(1-a)^2} - a}{(g\chi)(1-a)^2}, \quad (7)$$

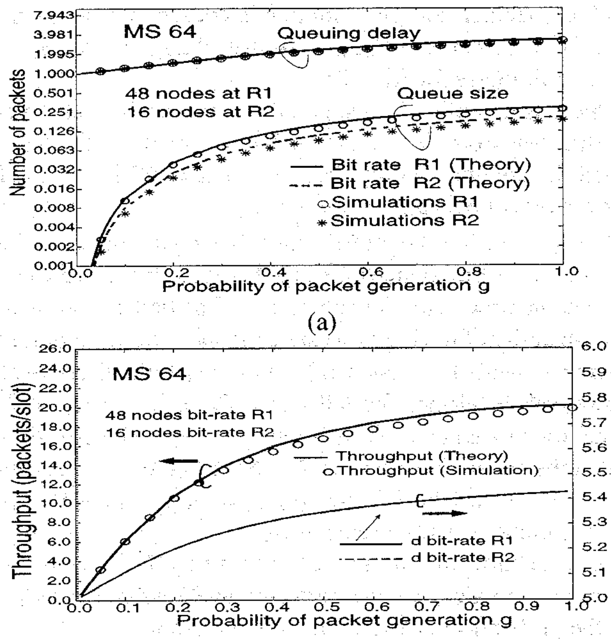

(a)

(b)

Figure 4: a) Queueing delay and Queue size in number of cells vs. g for Manhattan Street and ShuffleNet topologies. b)Throughput and Total network cell delay in number of hops vs. g for Manhattan Street with 48 nodes at bit rate R1 and 16 nodes at bit rate R2.

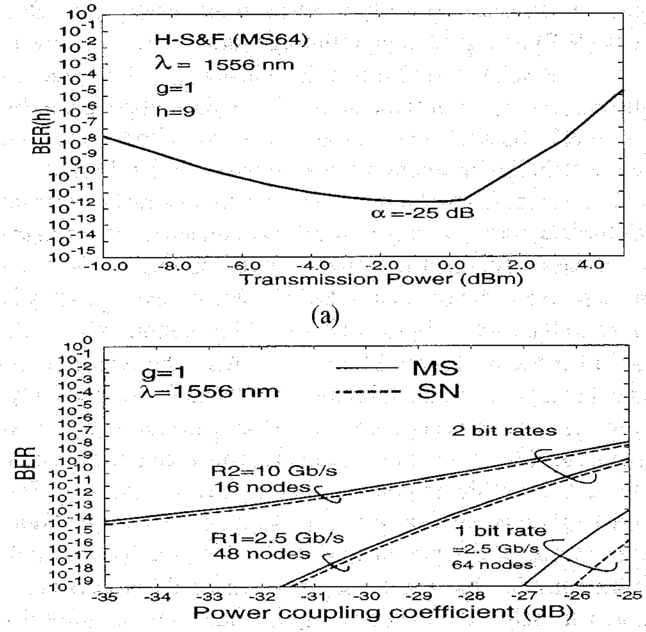

(a)

(b)

Figure 5: a) Conditioned BER(h) versus transmission power at hop number 9, **g=1**. b) BER versus power coupling coefficient α for g=1.

and the normalized transit delay of an R1 test cell is $d = H(1+\frac{D_{b-R1}\rho_{R1}}{W})$, where $\rho_{R1} = \frac{1}{2}u(1-a)(1-P_{dc})^2(P_{p-R2} + \frac{P_{p-R1}}{2})(P_{n-R1})$ is the probability of buffering an R1 test cell. Similarly the transit delay d of an R2 cell can be computed substituting the corresponding D_{b-R2} and ρ_{R2}. The queue size and queueing delay for R1 and R2 bit rate submodules are obtained using eqs. for Q_b and D_b substituting the respective μ and β probabilities.

Fig. 4a shows the average queue size and average queueing delay in number of cells of a MS topology with 64 nodes. The average queue size is smaller than 1 cell and the average queueing delay is lower than 4 cells. Observe that theory and simulation results show a good agreement. Since SN topology (B-P) performs similarly, we only considered MS. Fig. 4b shows throughput and average transit delay versus probability of cell generation. Observe that due to deflections the throughput is slightly lower compared to the one in Fig. 3. Also, the average normalized delay d increases (0.4 hops at g=1) due to deflection of cells.

The simulations statistics of the two bit rate communication network were obtained computing the average of queue size, queuing delay and throughput from 10,000 different uniformly distributed random locations of the R1 and R2 submodules. The reason is that the teletraffic performance depends on the location of the R1 and R2 submodules. All simulation statistics were collected for 30,000 clock cycles, after discarding 10,000 initial cycles to allow for transients to die out.

4. TRANSMISSION RESULTS

In multi-hop networks the BER is obtained by conditioning the BER(h) on the number of hops **h**, where **h** is a random variable, taken by a typical cell as $BER = \sum_{h=1}^{\infty} BER(h)\, P(h)$ [14]. The hop distribution P(h) [3] depends on network topology, routing, and load, while the conditional BER(h) depends on the *traffic load* and the optical characteristics of the network [5].

We analyzed a network with four channels in the range of 1550 nm to 1556 nm, with 2 nm channel separation. DEMUX with adjacent signal inter-band crosstalk of -30 dB, and a 2x2 crossbar optical switch with coupling power coefficient α between -25 dB and -35 dB are assumed. Filters at the output of the main switch (see Fig. 1) have a transfer function $T(\Delta\lambda)$= -17 dB. We represent each amplifier by using the spectrally resolved numerical model of [15] with a forward pumping scheme. The absorption and gain parameters are the same as those of fiber 2a in [16] with a length of 20 m and a pump power of 50 mW. Thus, it is assumed that the EDFA's are operating in the saturated regime. A bandwidth of 125 GHz is used to resolve the effect of ASE spectrum. The optical filter at the receiver has a 0.2 nm bandwidth and the electrical filter has a 2.5 GHz or 10 GHz bandwidth depending on the kind of node (N_{R1} or N_{R2}). We assumed a fiber with dispersion coefficient D_c =1 ps/km-nm, a loss coefficient of 0.2 dB/km, an internode distance of 15 km, a total node loss of 12.5 dB. The optical amplifiers are located at the output of each node.

We used a semi-analytical method [5], [17] to determine the error rate given that the path length **h** is known. Fig. 5a shows

	MS, H-S&F B-P	MS, H-S&F N-P	MS, H-S&F 2BR/B-P	SN, H-S&F B-P	SN, H-S&F N-P	SN, H-S&F 2BR/B-P
Transit delay d at g=1	5	∞ (saturation)	5.4	4.7	∞ (saturation)	5.1
Throughput	good	best	good	good	imbalance	good
Average Queue size	< 1 slot	saturation at g>0.95	< 1 slot	< 1 slot	imbalance at g>0.7	< 1 slot
Average Queueing delay	< 4 slots	saturation at g>0.95	< 4 slots	< 4 slots	imbalance at g>0.7	< 4 slots
BER, α=-25 dB α=-27 dB	$<10^{-9}$	$<10^{-9}$	$<10^{-9}$ R1 $<10^{-9}$ R2	$<10^{-9}$	----	$<10^{-9}$ R1 $<10^{-9}$ R2
Buffer Imbalance	NO	PARTIAL	NO	NO	YES	NO

Table1:Summary of results

the conditional BER(h) for hop number 9 versus transmission power at **g=1** for the channel at 1556 nm, the one with the worst gain. Results are shown for MS topology with a coupling coefficient of α=-25 dB and a bit rate of 2.5 Gb/s. The main impairments considered to compute BER(h) are intraband crosstalk and ASE noise. For low transmission power the predominant beat noise is signal-ASE that increases with bit rate and for high transmission powers the signal-crosstalk beat dominates, a noise that is bit rate independent [5], [17].

Fig. 5b shows BER results for a network of 64 nodes. Note that BER when all nodes transmit at R=2.5 Gb/s is below 10^{-9} for any α. Results for H-S&F (one bit rate) are for N-P, however B-P performs very similar to N-P. Also Fig. 5b shows results for B-P and dual bit rate communication, when 48 nodes use bit rate $R1 = 2.5$ Gb/s and 16 nodes use bit rate $R2 =$ 10 Gb/s. In this case the BER of 2.5 Gb/s nodes deteriorates because of possible cell deflections and the BER of 10 Gb/s nodes is worse because of cell deflections and higher bit rate. However, the BER is reasonably low for values of α below -27 dB. The curves were computed neglecting electronic *regeneration* of buffered cells, and are thus upper bounds on the actual BER values.

5. CONCLUSIONS

We presented a node architecture with routing buffers. Cells are stored just in the case of conflict to avoid deflection, otherwise they traverse the node without opto-electronic conversion (*transparent* cut-through [6] routing). Table 1 summarizes the results of this analysis. It is shown that cell correlation is much more severe in SN64 than in MS64. When locally generated cells have access priority, internal buffers can reach saturation at high loads ($g > 0.95$) for MS and ($g > 0.7$) for SN topologies. Our results show that in terms of throughput, N-P H-S&F performs better than B-P H-S&F. In terms of transit delay, B-P H-S&F performs better than N-P H-S&F at high traffic loads. Also, the results show that under SN and MS topologies with 64 nodes the BER is always lower than 10^{-9} assuming no regeneration of a test cell, and one bit rate communication scheme. Moreover, it is shown that with a combination of deflection routing and hybrid store-and-forward the network can accommodate communication with two different bit rates.

References

[1] N. F. Maxemchuk, "Comparison of deflection and store-and-forward techniques in the manhattan street and shuffle-exchange networks," in *Proc. IEEE INFOCOM '89*, pp. 800–809, Apr. 1989.

[2] R. Krishnan and N. F. Maxemchuk, "Is there life beyond linear topologies? a comparison of DQDB and the manhattan street network," in *Proc. IEEE INFOCOM'93*, pp. 690–698, 1993.

[3] F. Forghieri, A. Bononi, and P. Prucnal, "Analysis and comparison of hot-potato and single-buffer deflection routing in very high bit rate optical mesh networks," *IEEE Trans. on Commun.*, vol. 43, no. 1, pp. 88–98, January 1995.

[4] E. L. Goldstein, L. Eskildsen, and A. Elrefaie, "Performance implications of component crosstalk in transparent lightwave networks," *IEEE Photon. Technol. Lett.*, vol. 6, no. 5, pp. 657–660, 1994.

[5] G. A. Castañón, O. K. Tonguz, and A. Bononi, "BER performance of multi-wavelength optical cross-connected networks with deflection routing," *IEE Proc.-Communications*, vol. 144, no. 2, pp. 114–120, April 1997.

[6] P. Kermani and L. Kleinrock, "Virtual cut-through: a new computer communication switching technique," *Computer Networks*, vol. 3, no. 4, pp. 267–286, 1979.

[7] N. F. Maxemchuk, "Regular mesh topologies in local and metropolitan area networks," *AT&T Tech. J.*, vol. 64, no. 7, pp. 1659–1685, Sept. 1985.

[8] M. Eisenberg and N. Mehravari, "Performance of the multichannel multihop lightwave network under nonuniform traffic," *IEEE J. Select. Areas Commun.*, vol. 6, no. 7, pp. 1063–1078, August 1988.

[9] A. K. Choudhury and V. O. K. Li, "An approximate analysis of the performance of deflection routing in regular networks," *IEEE J. Select. Areas Commun.*, vol. 11, no. 8, pp. 1302–1316, October 1993.

[10] A. G. Greenberg and J. B. Goodman, "Sharp approximate models of deflection routing in mesh networks," *IEEE Trans. Commun.*, vol. 41, no. 1, pp. 210–223, Jan. 1993.

[11] L. Kleinrock, *Queueing Systems, Vol. 1: Theory*. New York: Wiley, 1975.

[12] A. S. Acampora and A. Shah, "Multihop lightwave networks: a comparison of store-and-forward and hot-potato routing," *IEEE Trans. on Commun.*, vol. 40, pp. 1082–1090, June 1992.

[13] A. Bononi and P. Prucnal, "Analytical evaluation of improved access techniques in deflection routing networks," *IEEE/ACM Transactions on Networking*, vol. 4, no. 5, pp. 726–730, October 1996.

[14] A. Bononi, F. Forghieri, and P. Prucnal, "Design and channel constrain analysis of ultrafast multihop all-optical networks with deflection routing employing solitons," *IEEE J. Lightwave Technol.*, vol. 11, no. 12, pp. 2166–2176, Dec. 1993.

[15] C. R. Giles and E. Desuvire, "Modeling erbium-doped fiber amplifiers," *IEEE J. Lightwave Technol.*, vol. 9, no. 2, pp. 271–283, Feb. 1991.

[16] C. R. Giles, C. Burrus, D. DiGiovanni, N. Dutta, and G. Raybon, "Characterization of erbium-doped fiber and application to modeling 980-nm and 1480-nm pumped amplifiers," *IEEE Photon. Technol. Lett.*, vol. 3, pp. 363–365, 1991.

[17] G. A. Castañón, O. K. Tonguz, and A. Bononi, "Transmission performance of transparent multi-wavelength optical cross-connected networks," in *IEEE Symposium on Computers and Communications (ISCC'97)*, vol. 1, pp. 323–329, 1-3 July, 1997. Also available at http://www.acsu.buffalo.edu/~castanon/publications.html.